Title

The cell wall of *Arabidopsis thaliana* influences actin network dynamics

Authors

Tolmie, A. F.[1], Poulet, A.[1 3], McKenna, J. F.[1], Sassmann, S.[2], Graumann, K.[1], Deeks, M.[2], Runions, J.[1]*

1 Department of Biological and Medical Sciences, Oxford Brookes University, Headington Campus, Oxford OX3 0BP, UK

2 Biosciences, College of Life and Environmental Sciences, University of Exeter, Exeter EX4 4QD, UK

3 Present address: Department of Biostatistics and Bioinformatics, Rollins School of Public Health, Emory University, Atlanta, Georgia 30322, USA

* Corresponding author

(12084313@brookes.ac.uk), (pouletaxel@gmail.com), (josephmckenna@brookes.ac.uk), (s.sassmann@exeter.ac.uk), (kgraumann@brookes.ac.uk), (M.Deeks@exeter.ac.uk), (jrunions@brookes.ac.uk).

Corresponding author is Runions, J: 01865 483964

Date of resubmission: **14/06/17**

Number of figures: **4**

Number of tables: **3**

Word count: **5624 words**

Number of supplementary items: **7**

Running title

Cell wall affects actin cytoskeleton dynamics in *A. thaliana*

Highlight

Actin cytoskeleton dynamics, as quantified with two new image analysis tools, were reduced in plasmolysed cells and cells treated with isoxaben to disrupt cell wall structure.

Abstract

In plant cells, molecular connections link the cell wall-plasma membrane-actin cytoskeleton to form a continuum. It is hypothesised that the cell wall provides stable anchor points around which the actin cytoskeleton remodels. Here we use live cell imaging of fluorescently labelled marker proteins to quantify the organisation and dynamics of the actin cytoskeleton and to determine the impact of disrupting connections within the continuum. Labelling of the actin cytoskeleton with FABD2-GFP resulted in a network composed of fine filaments and thicker bundles that appeared as a highly-dynamic remodelling meshwork. This differed substantially from the GFP-Lifeact-labelled network that appeared much more sparse with thick bundles that underwent 'simple movement', in which the bundles slightly change position, but in such a manner that the structure of the network was not substantially altered during the time of observation. Label-dependent differences in actin network morphology and remodelling necessitated development of two new image analysis techniques. The first of these, *Pairwise image subtraction* , was applied to measurement of the more rapidly-remodelling actin network labelled with GFP-FABD2 while the second, *Cumulative fluorescence intensity*, was used to measure bulk remodelling of the actin cytoskeleton when labelled with GFP-Lifeact. In each case, these analysis techniques show that the actin cytoskeleton has a decreased rate of bulk remodelling when the cell wall-plasma membrane-actin continuum is disrupted either by plasmolysis or with isoxaben, a drug that specifically inhibits cellulose deposition. Changes in the rate of actin remodelling also affect its functionality as observed by alteration in Golgi body motility.

Keywords

actin, cytoskeleton, cell wall, isoxaben, plasmolysis, image analysis, quantification, remodelling.

Abbreviations

AGP – Arabinogalactan protein

a.u. - Arbitrary units

BRI - Bulk Remodelling Index

CESA - Cellulose synthase A

CFI - Cumulative fluorescence intensity

CSC - Cellulose Synthase Complex

GFP - Green fluorescent protein

FABD2 - Fimbrin actin binding domain 2

PLD – Phospholipase D

SD - Standard deviation

SEM - Standard error of mean

ST - Sialyl transferase

WAK – Wall-associated kinase

Introduction

Plant cells are surrounded by a primary cell wall composed of carbohydrates and proteins which provides structural support and barrier-like defences (Cosgrove, 2005). Underlying this is the plasma membrane, which acts as an interface between the cell wall and cytoplasm and which is appressed against the cell wall by turgor pressure. Seifert and Blaukopf (2010) hypothesised that this physical pressure causes a 'mechanical connection' between the cell wall and plasma membrane allowing efficient signalling about cell wall integrity. This is a complicated relationship as proteins inserted into the outer leaflet of the plasma membrane can be immobilised by the cell wall and if plant cells are plasmolysed it causes lateral mobility of these proteins within the plasma membrane to increase (Martinière *et al.*, 2012). Links also exist that span the plasma membrane from the cell wall to the cytoskeleton creating what has been termed the "cell wall-plasma membrane-cytoskeleton" continuum (Kohorn, 2000; Baluska *et al.*, 2003; McKenna *et al.*, 2014; Liu *et al.*, 2015).

The actin cytoskeleton is important for many cellular processes and, with regard to the cell wall, it is important for trafficking vesicles containing CELLULOSE SYNTHASE A proteins (CESAs) to the cell periphery (Sampathkumar *et al.*, 2013). Indeed, the *act2-act7 Arabidopsis thaliana* mutant has been shown to have decreased cellulose levels, uneven cell wall thickness and increased lifetimes of CESAs at the plasma membrane (Sampathkumar *et al.*, 2013). In addition the actin cytoskeleton is involved in the motility of Golgi bodies, (Boevink *et al.*, 1998; Nebenfuhr *et al.*, 1999) and in the secretion of pectins and hemicelluloses which are delivered to the cell wall by vesicles moving along actin bundles (Golumb *et al*., 2008; Peremyslov *et al*., 2012; Wilson *et al*., 2015). However, the influence of the cell wall upon the actin cytoskeleton remains to be elucidated.

A. thaliana seems to lack homologues for many of the genes that are involved in linking the extracellular matrix to the actin cytoskeleton in animal cells, for example integrins (Baluska *et al.*, 2003; Meagher and Fechheimer, 2003). Integrins and cadherin complexes found in mammalian cells are thought to be too complex or tightly bound to quickly dissociate under hyper-osmotic stress conditions and this is considered a possible reason for their absence in plants (Baluska *et al.*, 2003). The function of the *A. thaliana* protein AT14A remains unknown, but it is considered to be integrin-like and it has been shown to be able to regulate organisation of both the cell wall and the cytoskeleton (Lu *et al.*, 2012).

There are several protein families hypothesised to be part of the cytoskeleton-plasma membrane-cell wall continuum: wall-associated kinases (WAKs), arabinogalactan proteins (AGPs), pectins, formins, class VIII myosins, phospholipase D (PLD) and callose synthases all play a role (Kohorn, 2000; Baluska *et al.*, 2003; Gardiner and Marc, 2013; Park and Nebenfuhr, 2013). Baluska *et al.* (2003) hypothesised that class VIII myosins and callose synthases might interact and they highlighted dramatic actin cytoskeleton rearrangement during callose deposition around the site of pathogen infection.

In this study we used two of the most common markers for live cell imaging of the actin cytoskeleton in *A. thaliana*: GFP-FABD2, the second actin binding domain of Fimbrin1 from *A. thaliana* and GFP-Lifeact, which comprises the first 17 amino acids from ABP140, an actin-binding protein from *Saccharomyces cerevisiae* (Kovar et al., 2000; Sheahan et al., 2004; Ketelaar et al., 2004; Riedl et al., 2008). van der Honing (2011) examined some of the differences between FABD2 and Lifeact and found that Lifeact labelled fine, very dynamic filamentous-actin in the subapical region of root hair cells, unlike FABD2; but that actin re-organisation was reduced in Lifeact-tagged cells relative to in FABD2-tagged cells. When fluorescence recovery after photobleaching (FRAP) was performed on both GFP-FABD2-, and GFP-Lifeact-tagged actin networks, GFP-Lifeact-tagged actin was shown to be more dynamic (reduced half-time of recovery) which the authors suggested was due to Lifeact's lower affinity for actin filaments (Sheahan et al., 2004; Smertenko et al., 2010; van der Honing et al., 2011). In addition, Rochetti (2014) showed that when Lifeact is expressed in a cell, the velocity of Golgi bodies is reduced and their movement pattern altered. All this suggests that FABD2 and Lifeact either cause two slightly different actin networks to be visualised, or more likely, that they affect actin cytoskeleton morphology and remodelling differentially (van der Honing *et al.*, 2011).

The cell wall-plasma membrane-cytoskeleton continuum is a complex structure in which the effect of the cell wall on structuring of the actin cytoskeleton network has not been specifically investigated. To that end, this study employed newly developed image analysis techniques (*Pairwise image subtraction* and *Cumulative frequency intensity*) to quantify global cellular changes in actin cytoskeletal dynamics (bulk remodelling) instead of individual events such as annealing and severing. Specifically, this study aimed to investigate the influence of the cell wall on the spatio-temporal organisation and dynamics of the actin cytoskeleton when tagged

with either GFP-FABD2 or GFP-Lifeact. Plasmolysis and treatment with isoxaben were used to perturb the cell wall-plasma membrane interface. Isoxaben specifically interferes with CESA3 and CESA6 and inhibits cellulose biosynthesis by stopping the incorporation of glucose into cellulose microfibrils (Scheible *et al.*, 2001; Desprez *et al.*, 2002; Sethaphong *et al.*, 2013; Tateno *et al.*, 2016). It leads to the majority of Cellulose Synthase Complexes (CSCs) being removed from the membrane within 20 min from the start of treatment (Paredez *et al.*, 2006). In addition, Golgi motility was quantified to assess actin network functionality, as previously published by Akkerman *et al.* (2011).

Materials and Methods

A. thaliana growth

A. thaliana Columbia-0 plants were grown on soil (Levington's F2 Seed and Modular compost) treated with 0.2 g/L Intercept 70WG for one week in 16 h light – 8 h dark and then for three weeks in a greenhouse at 18 h light – 6 h dark. Three stably transformed, homozygous lines were grown: 35S::GFP-Fimbrin Actin Binding Domain 2 (GFP-FABD2) (Sheahan *et al.*, 2004; Ketelaar *et al.*, 2004), 35S::GFP-Lifeact (Smertenko *et al.*, 2010) and 35S::Sialyl Transferase transmembrane domain (ST-GFP) (Saint-Jore, 2001).

Assays

A 0.5 cm^2 section was cut from rosette leaves five, six, seven or eight of mature *A. thaliana* plants, approximately 3-4 weeks old. For the plasmolysis assay, cells were plasmolysed in 0.6 M mannitol for 30 min and mounted in the same solution. Plasmolysed leaf sections that had not been imaged were rinsed in dH_2O and then incubated for a further 30 min in dH_2O and finally mounted in dH_2O (re-hydrated samples). Non-treated control leaves had no incubation at all and were mounted in dH_2O.

For the isoxaben assay, leaf sections were incubated in ½ MS plus 1% MES at pH 5.7 for 1 hour or 4 hours with either 20 µM isoxaben or 0.01% dimethyl sulfoxide as a control.

Confocal microscopy

Cells were mounted in incubation solution or water if not treated; imaging was carried out using an inverted (Axio-Vert) Zeiss LSM 510 confocal microscope with a 63x 1.4NA oil immersion objective. Fluorescence was excited with an Argon 488 nm laser and emitted fluorescence was collected using a band pass filter (505-550 nm).

Only leaf epidermal pavement cells were imaged. Cells that stably-expressed fluorescence markers for the actin cytoskeleton were imaged using a region of interest of 200 by 150 pixels (28 by 21 µm). A 4D imaging approach was used to capture cytoskeletal dynamics in 3D projected images. Z-stacks 4 µm thick, with 1 µm intervals between slices were made 20 times with no delay between successive stacks, so that each time-series has a duration of 105 s (5.5 s between each z-stack). Cells that stably-expressed a fluorescence marker for Golgi bodies were imaged using a region of interest of 200 by 150 pixels as 2D images rather than 3D and each time-series had 200 time-frames, no delay between time-frames. These time-series had a duration of 90 s (0.46 s between time-frames).

Tracking Golgi bodies

Volocity software [PerkinElmer, Massachusetts, USA] was used to track Golgi body movement as has been described previously (Runions *et al.*, 2006; Sparkes *et al.*, 2008; Martinière *et al.*, 2011; Rocchetti *et al.*, 2014).

Image analysis tools

Due to the differences in morphology and behaviour between the two markers used to visualise the actin cytoskeleton (Figure 1; Supplemental movies 1-2), two image analysis techniques were devised for measuring bulk remodelling within the actin cytoskeleton. These were called '*Pairwise image subtraction*' which was used for analyses of the GFP-FABD2 label, and '*Cumulative fluorescence intensity*' which was used to analyse the GFP-Lifeact label.

Pairwise image subtraction for GFP-FABD2 labelled data collected as described above was done using ImageJ (Rasband, 1997-2016) (Figure S1). 'Maximum intensity projection' was used to project each 3D time-frame of a timeseries. The resulting 2D image was then manually thresholded; the thresholds were set above detector noise and cytosolic signal. The dataset was cropped to make it the size of the region of interest that was used when imaging; each

time-frame contained 30,000 pixels. A 0.2 median filter was used to reduce any remaining noise. The time-frames in each time-series were then sequentially subtracted using the 'Image Calculator' function starting with time-frame '2' minus time-frame '1' and so on (TF3-TF2, TF4-TF3... TF20-TF19). The 'Color Pixel Counter' plugin was then used to count the number of pixels in the resultant subtracted image that contained fluorescence intensity >1, and all of the pixels with intensity values >1 in the first image of each pair (http://imagejdocu.tudor.lu/doku.php?id=plugin:color:color_pixel_counter:start) (Rasband, 1997-2016).

The number of pixels containing fluorescence in the subtracted image was expressed as a proportion of the number of pixels containing fluorescence in the first time-frame of each pair and this was called the bulk remodelling index (BRI):

$$BRI = \#\ pixels\ I{>}1_{subtracted\ image} / \#\ pixels\ I{>}1_{first\ image}$$

Where 'I' is fluoresence intensity

The resulting 19 BRI values for each timeseries were used to calculate mean BRI for which small values (BRI<0.5) indicate a relatively static network while large values (BRI>0.5) indicate a network that has undergone relatively more remodelling during the time of observation.

Cumulative fluorescence intensity for GFP-Lifeact labelled data collected as described above was done using ImageJ (Rasband, 1997-2016) (Fig. S2-S3). The datasets were initially treated as described above for *Pairwise image subtraction* until they were filtered using the 0.2 median filter and then they were treated as follows. After filtering the datasets were converted to 8-bit and processed using the batch-process function in the '*Cumulative fluorescence intensity*' plugin. For each timeseries every pixel in each time-frame with fluorescence intensity value (I) of '1' or higher ('0' is black and '255' is the highest intensity) was assigned the value '1', while all pixels with the value '0' remained as '0'. Then, at each pixel position for an entire timeseries, the '*Cumulative fluorescence intensity*' plugin sums the I values>1 to produce a number that we termed the Cumulative fluorescence intensity (CFI), i.e. with a region of interest of 200x150 pixels and 20 time frames the CFI for the first pixel position (0,0) is calculated as:

$CFI_{(0,0)} = \sum_{t=1}^{20} I = 1$

This was repeated for each pixel position to (199,149).

To remove residual noise from the data, the calculated CFI was reduced by '1' at each pixel location before subsequent calculations were made. For each timeseries, the number of pixel positions at each possible CFI (0-19) was calculated. This resulted in a histogram illustrating the proportion of highly dynamic actin (low CFI) to relatively static actin (high CFI) in a 4D data set. The number of pixels at each possible CFI in plasmolysed and re-hydrated samples were expressed as the ratio between the treatment and control. For our purposes, we analysed the proportion of pixel locations in the highest FIV categories as an estimate of the relative immobility in the actin cytoskeleton between treatments.

CFI<4 was considered dark background with little actin cytoskeleton occupancy during the observation. A relatively large proportion of pixels at small CFI (CFI = 5-10) indicate a dynamic network that has undergone rapid remodelling as fluorescence was only peridically detected in the same position. Conversely, a relatively large proportion of pixels at large CFI (CFI = 11-19) indicates a static network as fluorescence has repeatedly been detected in the same position implying that the network does not remodel.

Statistical analyses

Datasets contained approximately 30 cells divided between seven plants unless otherwise stated. Data were analysed using GraphPad Prism software [GraphPad Software Inc., California, USA]; the statistics used were One-way ANOVA, Kruskal-Wallis or unpaired t-tests with Welch's correction, depending on the spread of the data as shown by histograms (data not shown).

Box plots were used for some data, in each case the top line of the box represents the upper quartile, below this line is 75% of the data points. The middle line represents the median, the middle-most value and the lowest line of the box represents the lower quartile beneath which

is 25% of the data points. The Tukey whiskers represent 1.5 times the upper interquartile range (upper whisker) and 1.5 times the lower interquartile range (lower whisker).

Results

Changes in actin organisation

In non-treated (control) cells stably-expressing GFP-FABD2 the actin cytoskeleton displayed a range of morphologies, but most common was a close-knit meshwork of filaments with few large bundles and very few visible thin bundles. However, in plasmolysed cells there were large bundles and less of a meshwork with brighter fluorescence. Cells that had been plasmolysed and then rehydrated showed lower levels of fluorescence, but the network appeared similar to control cells except more large bundles were observed (Fig. 1).

In non-treated (control) cells stably-expressing GFP-Lifeact the actin cytoskeleton displayed a sparse network of large bundles. Plasmolysed cells seemed to have a similar type of network, but the bundles appeared less straight. In cells that had been plasmolysed and then rehydrated the GFP-Lifeact marked actin cytoskeleton appeared similar to those in control cells (Fig. 1).

Both of the image analysis techniques created measure bulk remodelling, or changes over time in the actin cytoskeleton network. The different behaviours of the actin cytoskeleton as visualised with the two markers mean that *Pairwise image subtraction* results in a useful quantification of actin bundle dynamics within GFP-FABD2-tagged networks, but not within the GFP-Lifeact-tagged networks in which lateral drift of the entire network without apparent remodelling returns a falsely high Bulk Remodelling Index.

On the other hand, the *Cumulative fluorescence intensity* technique works effectively with the more sparse GFP-Lifeact-tagged networks because the large, slowly remodelling bundles of actin rarely move to reoccupy a vacated pixel location thus returning a true fluorescence intensity value at each location. GFP-FABD2 labelling of the actin cytoskeleton produces a more dense meshwork of microfilaments so *Cumulative fluorescence intensity* returns falsely high CFI values indicating a more static network because bundles often remodel back into areas that other bundles had vacated.

Disruption of the cell wall-plasma membrane interface by plasmolysis causes a reduction in remodelling of the actin cytoskeleton

As a first step towards investigating the influence of the cell wall on the actin cytoskeleton, we chose to carry out plasmolysis on *A. thaliana* abaxial epidermal pavement cells using mannitol. Cells stably expressing GFP-FABD2 were either plasmolysed with 0.6 M mannitol for 30 min or left untreated as a control (Figure 1-A). The *Pairwise Image Subtraction* results indicate not only that the actin cytoskeleton displays different morphologies depending on the marker used (as shown by other studies, such as van der Honing, 2011), but that the organisational alterations as a consequence of plasmolysis are also marker dependant. Plasmolysed cells showed significantly decreased bulk remodelling compared to non-treated cells (BRI mean ± SD; non-treated control = 0.56 ± 0.06 vs plasmolysed = 0.53 ± 0.04; $p < 0.0001$), suggesting a more static network in cells that lack an intact cell wall-plasma membrane interface (Figure 1-B and Table 1).

However, it is possible that as plasmolysis has a tissue-wide effect the observed change was due to pleiotropic effects. Therefore to determine if this effect was permanent or whether it could be reversed if the cell wall-plasma membrane contact was re-established, plasmolysed cells were rehydrated (BRI 0.60 ± 0.09; $p < 0.0001$; Figure 1 A-B and Table 1).

This experiment was repeated with cells stably expressing GFP-Lifeact, but analysed using *Cumulative fluorescence intensity* (Figure 1-C and Tables 2 and S1). The proportion of the highest CFI values was significantly higher in the plasmolysed sample compared to the non-treated control, indicating a reduction in cytoskeletal remodelling after plasmolysis (Tables 2 and S1). There were no significant differences for any CFI level when the rehydrated cells were compared to the non-treated cells ($p > 0.05$; Figure 1-D).

Using both *Pairwise image subtraction* and *Cumulative fluorescence intensity* a decrease in bulk remodelling in GFP-FABD2-, and GFP-Lifeact-tagged actin networks was observed during plasmolysis (Tables 1 and 2). This suggests that one consequence of plasmolysis is a change in the spatio-temporal dynamics of the actin cytoskeleton and that reversing the effects of plasmolysis by rehydration made the network behave more like the non-treated networks (Figure 1).

Golgi body movement as a proxy for actin cytoskeleton dynamics

Tracking Golgi body motility can be used as a proxy for the function of the actin cytoskeleton as their motility is actin-myosin dependent (Boevink *et al.*, 1998; Nebenfuhr *et al.*, 1999). It has been shown that Golgi bodies move differently on different actin cytoskeleton morphologies and also that actin markers affect their mobility differentially (Akkerman *et al.*, 2011, Rocchetti *et al.*, 2014). Therefore, we used an *A. thaliana* line that stably expressed ST-GFP, a marker for Golgi bodies (Saint-Jore, 2001) and analysed their motility using Volocity software.

Golgi bodies move slower in plasmolysed cells compared to non-treated cells (Golgi velocity - mean ± standard error of mean: non-treated = 0.69 ± 0.02 µm/s vs plasmolysed = 0.52 ± 0.02 µm/s; $p<0.001$; Figure 2-A), whereas re-hydrating plasmolysed cells resulted in Golgi bodies moving at the same speed as in non-treated cells, (rehydrated = 0.77 ± 0.02 µm/s; $p > 0.05$; Figure 2 and Table 3).

The displacement rate describes the length of time taken for an object to travel between two points measured as a straight line. Golgi bodies took a longer time to travel between two points in plasmolysed cells compared to non-treated cells. Whereas again, re-hydrating plasmolysed cells resulted in Golgi bodies moving at the same rate as in non-treated cells (Figure 2 and Table 3). The Meandering Index (MI) is a ratio (displacement rate divided by average velocity) that describes the complexity of the movement undergone by an object: at values close to 1, the object has moved in a relatively straight line, whilst the closer the index value is to 0, the more complicated and convoluted the movement. Golgi bodies tended to move in a more complicated manner in plasmolysed cells compared to non-treated cells, but upon re-hydration they reverted to a similar type of movement as observed in non-treated cells (MI -mean ± SD: non-treated = 0.33 ± 0.25 vs plasmolysed = 0.28 ± 0.26, $p<0.001$, and vs re-hydrated = 0.35 ± 0.27, $p > 0.05$; Figure 2-C and Table 3).

Golgi bodies remained in the field of view for a longer duration in plasmolysed cells compared to non-treated cells, suggesting slower, smaller movements (Figure 2 and Table 3). Interestingly, Golgi bodies also remained in the field of view for a longer duration in re-hydrated cells, which was unexpected, given the previous results.

In summary, Golgi body motility was altered by plasmolysis, perhaps indicating that alterations in the spatio-temporal dynamics of the actin cytoskeleton affect its function as a transport network (Figure 2 and Table 3).

Disruption of the cell wall by isoxaben causes a reduction in the remodelling of the actin cytoskeleton

We predicted that the observed changes in actin cytoskeletal dynamics in plasmolysed cells were due to the separation of the cell wall from the plasma membrane and therefore loss of the direct or indirect connections between cell wall and actin cytoskeleton. To determine whether this was specific to plasmolysis or whether it was a standard response to disruption at the cell wall-plasma membrane interface we treated cells with isoxaben. We also confirmed that this response is not a general reaction in to any abiotic stress by incubating cells at different temperatures (Fig. S4).

We imaged mature leaf pavement epidermal cells that stably expressed GFP-FABD2 to determine if isoxaben treatment affected bulk actin remodelling. Cells that stably expressed GFP-FABD2 were either mock-treated with DMSO or treated with 20 µM isoxaben for either 1 h or 4 h (Figure 3). At both time-points, the Bulk Remodelling Index (as measured by *Pairwise image subtraction*) in the treated samples was significantly reduced compared to the mock (BRI - mean ± SD: mock 1 h = 0.62 ± 0.06 vs 20 µM isoxaben-treated 1 h = 0.61 ± 0.06 and mock 4 h = 0.61 ± 0.06 vs 20 µM isoxaben-treated 4 h = 0.60 ± 0.05; $p < 0.01$ and $p < 0.001$, respectively; Figure 3). These results correlate with the data obtained from the plasmolysis experiment, demonstrating that interfering with the cell wall-plasma membrane interface reduces bulk remodelling of the actin cytoskeleton.

Discussion

Image analysis tools to quantify bulk remodelling of the actin cytoskeleton

We have focussed on quantifying bulk remodelling of the actin cytoskeleton and the effect of disrupting the cell surface continuum on actin network morphology and function. Bulk remodelling, in this sense, incorporates various individual processes of cytoskeletal change

including polymerisation, annealing and severing. This was measured as rates of change at the spatial and temporal scale in living cells using confocal microscopy with two fluorescent markers for the actin cytoskeleton: GFP-FABD2 and GFP-Lifeact (Sheahan *et al.*, 2004; Ketelaar *et al.*, 2004; Smertenko *et al.*, 2010). We applied different image analyses techniques in a marker-dependent manner. *Pairwise image subtraction* was used to analyse cells in which the actin cytoskeleton was marked with GFP-FABD2 and it returns a variable that we have called the Bulk Remodelling Index (BRI). Similarly, we have developed a technique called *Cumulative fluorescence intensity* which returns a variable that we call Cumulative fluorescence intensity (CFI) for each pixel location in 4D data sets and applied it to analyses of cells expressing GFP-Lifeact. Both BRI and CFI estimate the rate of bulk remodelling during timecourse recording of actin cytoskeleton. Each of these methods worked well for the specific actin marker in question but returned erroneous results when applied to the other actin marker. This interesting finding results from the previously characterised differences in cytoskeleton morphology and dynamic properties that marking with GFP-FABD2 and GFP-Lifeact impose upon the actin network.

When labelled with GFP-FABD2, the actin cytoskeleton appears as a denser meshwork of fairly dynamic microfilaments and bundles. *Pairwise image subtraction* is a robust technique that accurately describes the amount of change between timepoints when the observed change is isomorphic as occurs with GFP-FABD2 marking. However, when *Pairwise image subtraction* was applied to the GFP-Lifeact labelled actin cytoskeleton, a false impression of highly dynamic actin microfilaments and bundles resulted because of the cytoskeleton's peculiar lateral motion. When labelled with GFP-Lifeact, the actin network remains relatively unchanging relative to the GFP-FABD2 label except that lateral drift of the entire network structure occurs. This was considered an anisotropic form of lateral remodelling that proved to be much more convincingly quantified with *Cumulative fluorescence intensity*-based production of CFI-levels histograms for each data set. In this case, large numbers of pixel locations with high CFIs implied a more static network.

<u>Cell wall-plasma membrane interface disruption</u>

Despite this label-dependent morphological variation in the actin network structure, when the cells were plasmolysed the actin cytoskeleton as visualised with either GFP-FABD2 or GFP-

Lifeact displayed a reduced rate of remodelling. This reduction in the rate of remodelling was also seen in GFP-FABD2-labelled networks when cells were treated with the cellulose synthesis inhibitor, isoxaben.

Plasmolysis and isoxaben are different approaches to disrupting the cell wall-plasma membrane interface. Plasmolysis is a general effect that causes almost complete separation of the protoplasm from the cell wall apart from Hechtian strands that remain connected to both structures (Oparka, 1994). Conversely, isoxaben perturbs the molecular make-up of the cell wall, by specifically acting upon three of the CESA proteins found within the CSC and causing these large complexes to be removed from the plasma membrane (Tateno *et al.*, 2016).

Previous studies have investigated changes in the structure of the actin cytoskeleton in plasmolysed cells. Lang *et al.* (2014) monitored the actin cytoskeleton during the onset of plasmolysis and reported that actin filaments reorganise rapidly and when the cell was fully plasmolysed they observed many actin bundles. This suggests that as the protoplasm separates from the cell wall the actin cytoskeleton rapidly alters in structure, forming bundles that become stable as the cell becomes fully plasmolysed. Komis *et al.* (2002) thought that actin bundles mitigate the physical stresses caused by the deformation of the plasma membrane. Wojtaszek *et al.* (2007) and Lang *et al.* (2014) compared these bundle structures to the stress fibres found in animal cells; they, and Komis *et al.* (2002), suggest that the bundles are involved in maintaining the shape and regulating volume of the protoplast during plasmolysis. The mechanical properties of these 'stress fibre-like' actin bundles will be dependent on the proteins that cross-link the filaments: how tightly they bind them together and how much sliding can occur (Blanchoin *et al.*, 2014).

We found that the Bulk Remodelling Index was significantly reduced in both isoxaben-treated samples compared to their respective mock treatments. A short-duration incubation with isoxaben is not expected to significantly alter the structure of the cell wall (Martinière *et al.*, 2012). However, there will be small changes to the patterning of cellulose microfibrils as production of cellulose is halted. In mature cells this production is expected to be involved in maintenance of the cell wall (Martinière *et al.*, 2012). Wojtaszek *et al.* (2007) hypothesised that disrupting different cell wall components during plasmolysis would affect the actin cytoskeleton differently. This suggests that an interesting next step would be to treat cells

with cell-wall disrupting agents that act in different ways and that affect different cell wall components.

We suggest that there is a two-fold reason for the reduction in the rate of remodelling in the actin cytoskeleton when either the protoplasm is separated spatially from the cell wall, or the structure of the cell wall is altered. Firstly, if the actin bundles observed in plasmolysed cells are involved in supporting the protoplast structure, then they would need to be relatively rigid and static. Secondly, Martinière *et al.* (2011) suggested that the cell wall itself acts as a provider of stable anchor points for the dynamic actin cytoskeleton to remodel around, they used formin1 (AtFH1) as an example of a protein that binds both actin microfilaments and the cell wall and is involved in remodelling of the actin cytoskeleton (Figure 4).

Consequences to actin cytoskeleton function in cells with a perturbed 'cell surface continuum'

The motility of Golgi bodies was analysed in plasmolysed cells to determine if the reduced rate of remodelling observed in the actin cytoskeleton interfered with the functionality of the network. Golgi body motility is actin cytoskeleton and myosin dependant (Boevink *et al.*, 1998; Avisar *et al.*, 2009). We found that Golgi body motility in plasmolysed cells was altered in several respects relative to controls: reduced average velocity, reduced average displacement, reduced meandering index and increased number of time frames that Golgi bodies were present in the field of view. Interestingly, in *A. thaliana* seedlings a two hour incubation with isoxaben causes a reduction in Golgi body motility (Gutierrez *et al.*, 2009) thus suggesting that it is, indeed, the physical connection between actin cytoskeleton and the cell wall that regulates actin functionality.

Within approximately six min from the onset of plasmolysis, most of the CSCs are removed from the plasma membrane and localise to specific vesicles that interact with Golgi bodies (Crowell *et al.*, 2009). After 30 min of plasmolysis there are very few CSCs left in the plasma membrane and not only can CESA proteins be detected in vesicles, but the rate that they are delivered to the plasma membrane is dramatically decreased (Gutierrez *et al.*, 2009; Endler *et al.*, 2015). Interestingly, Gutierrez *et al.* (2009) also showed that osmotic stress reduced motility of Golgi bodies and endosomes, they concluded that osmotic stress affected

membrane trafficking in general. This is probably a consequence of the reduction in the rate of remodelling that we observed.

Golgi bodies have been shown to move faster on actin bundles than on fine filaments. For example, Martinière *et al.* (2011) over-expressed AtFH1 and observed a very dense meshwork of actin cytoskeleton composed of finer filaments with fewer bundles and they determined that Golgi bodies had reduced motility. In addition, Akkerman *et al.* (2011) imaged Golgi bodies moving on actin and found that they moved at greater speeds and in a more directional manner on actin bundles compared to on fine filaments. Geitmann and Nebenfuhr (2015) hypothesised that organelle speeds may be dependent on the number of myosins linking the organelle to the actin cytoskeleton. They go on to suggest that thicker bundles of actin filaments would allow more of these connections thus reducing drag from the cytosol and giving the opportunity for greater speeds (Geitmann and Nebenfuhr, 2015). It is therefore expected that an alteration in spatio-temporal dynamics of the actin cytoskeleton would cause a change in the motility of Golgi bodies.

The mechanism that causes this change in the motility of Golgi bodies in plasmolysed cells is so far unclear, although the viscosity of the cytoplasm itself may be altered during plasmolysis (Oparka, 1994). It could be that movement of Golgi bodies along bundled filaments is hampered by a physical aspect of the bundles, perhaps over-use or structural changes. Myosins may interact differently with bundles; perhaps actin bundles in plasmolysed cells are constructed differently to the usual bundles observed in cells, which somehow impedes these interactions. For example, stress fibres in animals cells are made from antiparallel arrangements of filaments (Blanchoin *et al.*, 2014). Moreover, it has been shown that in actin mutants, Golgi bodies may appear as they do in wild-type, but that they are surrounded by a large quantity of vesicles, presumably due to a lack of trafficking in an actin-impaired cell (Sampathkumar *et al.*, 2013).

There is the possibility that changes in the rate of actin cytoskeleton remodelling would also affect the microtubule cytoskeleton as it is known that they interact (Sampathkumar *et al.*, 2011). However, it would be difficult to accurately assess direct and indirect effects of the actin cytoskeleton on microtubules as the microtubule cytoskeleton is directly connected to and therefore affected by the cell wall (Szymanski and Cosgrove, 2009). In addition, the microtubule cytoskeleton seems to be involved in the ‘pausing’ of Golgi bodies as they move

around the cell (Nebenfuhr *et al.*, 1999, Crowell *et al.*, 2009), indeed, certain kinesins have been shown to be able to interact with Golgi bodies (Lu *et al.*, 2005, Zhu *et al.*, 2015).

Biological mechanisms, molecular regulation and general significance of a continuum between the cell wall and actin cytoskeleton

The next step would be to try to identify proteins that interact to maintain the structure of the 'cell surface continuum' and to obtain mutants of these in order to analyse the dynamics of the actin cytoskeleton. It would also be interesting to try to get a clear picture of the interaction between the actin and microtubule cytoskeletons, perhaps it will even be appropriate to consider the microtubule cytoskeleton a component of the 'continuum'.

Of the other protein families putatively involved in the 'continuum' the five WAKs proteins in *A. thaliana* are known to link to pectins in the cell wall, but also contain a kinase domain located in the cytoplasm (Kohorn and Kohorn, 2012). WAKs are thought to be part of the pathogen response and probably act as receptors for pectins and pectin fragments (Kohorn and Kohorn, 2012). Another family of proteins intimately linked to the cell wall are the AGPs. Sardar *et al.* (2006) treated cells with β-Yariv, a reagent that causes AGPs to aggregate into complexes and they observed that the microtubule and actin cytoskeletons were disturbed. Lastly, Pin-formed (PIN) proteins are generally considered to be plasma membrane localised but in plasmolysed cells they can be located at both the plasma membrane and the cell wall that was adjacent to the polar membrane domain (Feraru *et al.*, 2011). A good example of actin binding proteins that were not identified via homology searches is the Networked (NET) superfamily which was identified by screening a GFP-tagged cDNA expression library (Deeks *et al.*, 2012). NET3C can bind to VAP27, a protein which is a homologue of a yeast protein involved in endoplasmic reticulum-plasma membrane contact sites, they form a complex which can interact with both the actin and microtubule cytoskeleton (Wang et al., 2014).

Lastly, it would be very interesting not only to extend this analysis to other markers for the actin cytoskeleton and also to attempt to quantify remodelling within the microtubule cytoskeleton and the endoplasmic reticulum, but also to extend the analysis tools presented here technically, to allow analysis of networks in 3D rather than 2D. This would allow for increased resolution of the axial effects of cell wall influence on cytoskeletal remodelling.

To summarise, we have demonstrated that the cell wall in *A. thaliana* has an influence over the dynamics of the actin cytoskeleton using two new image analysis techniques developed during the course of this study. It opens the way for many interesting further experiments on the nature of the actin bundles formed during plasmolysis, or after perturbation of cell wall structure as well as identification of more of the proteins or protein complexes involved in linking the cell wall and the actin cytoskeleton to maintain the function of the cell surface continuum.

Supplementary data

Table S1. *Cumulative fluorescence intensity* data from plasmolysis experiments.

Fig. S1. Workflow for the *Pairwise image subtraction* analysis technique.

Fig. S2. Schematic of *Cumulative fluorescence intensity* analysis technique.

Fig. S3. Validation of *Cumulative fluorescence intensity* analysis using a modified 'bootstrapping' method.

Fig. S4. Temperature stress does not alter the dynamic remodelling of the actin cytoskeleton.

Supplemental Movie 1. Timeseries of GFP-FABD2 tagged actin cytoskeleton.

Supplemental Movie 2. Timeseries of GFP-Lifeact tagged actin cytoskeleton.

Acknowledgements

We thank Dr. Verena Kriechbaumer, Prof. David Evans and Prof. Chris Hawes for constructive comments during writing of the manuscript. This work was supported by Oxford Brookes University and the BBSRC though a Nigel Groome funding for AFT and AP, AP also funded by Blaise Pascal Université, BBSRC Responsive Mode Grant for JFM and JR [BB/K009370/1] and funding from the University of Exeter and BBSRC for MD and SMS.

References

AKKERMAN, M., OVERDIJK, E. J., SCHEL, J. H., EMONS, A. M. & KETELAAR, T. 2011. Golgi body motility in the plant cell cortex correlates with actin cytoskeleton organization. *Plant and Cell Physiology,* 52**,** 1844-1855.

AVISAR, D., ABU-ABIED, M., BELAUSOV, E., SADOT, E., HAWES, C. & SPARKES, I. A. 2009. A comparative study of the involvement of 17 *Arabidopsis* myosin family members on the motility of Golgi and other organelles. *Plant Physiology,* 150**,** 700-709.

BALUSKA, F., SAMAJ, J., WOJTASZEK, P., VOLKMANN, D. & MENZEL, D. 2003. Cytoskeleton-plasma membrane-cell wall continuum in plants. Emerging links revisited. *Plant Physiology,* 133**,** 482-491.

BLANCHOIN, L., BOUJEMAA-PATERSKI, R., SYKES, C. & PLASTINO, J. 2014. Actin dynamics, architecture and mechanics in cell motility. *Physiological Reviews,* 94**,** 235-263.

BOEVINK, P., OPARKA, K., SANTA CRUZ, S., MARTIN, B., BETTERIDGE, A. & HAWES, C. 1998. Stacks on tracks: the plant Golgi apparatus traffics on an actin-ER network. *The Plant Journal,* 15**,** 441-447.

COSGROVE, D. J. 2005. Growth of the plant cell wall. *Nature Reviews. Molecular Cell Biology,* 6**,** 850-861.

CROWELL, E. F., BISCHOFF, V., DESPREZ, T., ROLLAND, A., STIERHOF, Y. D., SCHUMACHER, K., GONNEAU, M., HOFTE, H. & VERNHETTES, S. 2009. Pausing of Golgi bodies on microtubules regulates secretion of cellulose synthase complexes in *Arabidopsis*. *The Plant Cell,* 21**,** 1141-1154.

DEEKS, M. J., CALCUTT, J. R., INGLE, E. K., HAWKINS, T. J., CHAPMAN, S., RICHARDSON, A. C., MENTLAK, D. A., DIXON, M. R., CARTWRIGHT, F., SMERTENKO, A. P., OPARKA, K. & HUSSEY, P. J. 2012. A superfamily of actin-binding proteins at the actin-membrane nexus of higher plants. *Current Biology,* 22**,** 1595-1600.

DEEKS, M. J., HUSSEY, P. J. & DAVIES, B. 2002. Formins: intermediates in signal-transduction cascades that affect cytoskeletal reorganization. *Trends in Plant Science,* 7**,** 492-498.

DESPREZ, T., VERNHETTES, S., FAGARD, M., REFREGIER, G., DESNOS, T., ALETTI, E., PY, N., PELLETIER, S. & HOFTE, H. 2002. Resistance against herbicide isoxaben and cellulose deficiency caused by distinct mutations in same cellulose synthase isoform CESA6. *Plant Physiology,* 128**,** 482-490.

ENDLER, A., KESTEN, C., SCHNEIDER, R., ZHANG, Y., IVAKOV, A., FROEHLICH, A., FUNKE, N. & PERSSON, S. 2015. A mechanism for sustained cellulose synthesis during salt stress. *Cell,* 162**,** 1353-1364.

FERARU, E., FERARU, M. I., KLEINE-VEHN, J., MARTINIÈRE, A., MOUILLE, G., VANNESTE, S., VERNHETTES, S., RUNIONS, J. & FRIML, J. 2011. PIN polarity maintenance by the cell wall in *Arabidopsis*. *Current Biology,* 21**,** 338-343.

GARDINER, J., MARC, J. 2013. Phospholipases may play multiple roles in anistropic plant cell growth. *Protoplasma,* 250, 391-395.

GEITMANN, A. & NEBENFUHR, A. 2015. Navigating the plant cell: intracellular transport logistics in the green kingdom. *Molecular Biology of the Cell,* 26**,** 3373-3378.

GOLOMB, L., ABU-ABIED, M., BELAUSOV, E., & SADOT, E. 2008. Different subcellular localizations and functions of *Arabidopsis* myosin VIII. *BMC Plant Biology,* 8, 1-13.

GOWRISHANKAR, K., GHOSH, S., SAHA, S., C, R., MAYOR, S. & RAO, M. 2012. Active remodeling of cortical actin regulates spatiotemporal organization of cell surface molecules. *Cell,* 149**,** 1353-1367.

GUTIERREZ, R., LINDEBOOM, J. J., PAREDEZ, A. R., EMONS, A. M. & EHRHARDT, D. W. 2009. *Arabidopsis* cortical microtubules position cellulose synthase delivery to the plasma membrane and interact with cellulose synthase trafficking compartments. *Nature Cell Biology,* 11**,** 797-806.

HIGAKI, T., KUTSUNA, N., SANO, T., KONDO, N. & HASEZAWA, S. 2010. Quantification and cluster analysis of actin cytoskeletal structures in plant cells: role of actin bundling in stomatal movement during diurnal cycles in *Arabidopsis* guard cells. *The Plant Journal,* 61**,** 156-165.

KETELAAR, T., ALLWOOD, E. G., ANTHONY, R., VOIGT, B., MENZEL, D. & HUSSEY, P. J. 2004. The actin-interacting protein AIP1 is essential for actin organization and plant development. *Current Biology,* 14**,** 145-149.

KOHORN, B. D. 2000. Plasma membrane-cell wall contacts. *Plant Physiology,* 124**,** 31-38.

KOHORN, B. D. & KOHORN, S. L. 2012. The cell wall-associated kinases, WAKs, as pectin receptors. *Frontiers in Plant Science,* 3**,** 88-93.

KOMIS, G., APOSTOLAKOS, P. & GALATIS, B. 2002. Hyperosmotic stress-induced actin filament reorganization in leaf cells of *Chlorophyton comosum*. *Journal of Experimental Botany,* 53**,** 1699-1710.

KOVAR, D. R., STAIGER, C. J., WEAVER, E. A. & MCCURDY, D. W. 2000. AtFim1 is an actin filament crosslinking protein from *Arabidopsis thaliana*. *The Plant Journal,* 24**,** 625-636.

KREPS, J. A., WU, Y., CHANG, H. S., ZHU, T., WANG, X. & HARPER, J. F. 2002. Transcriptome changes for *Arabidopsis* in response to salt, osmotic, and cold stress. *Plant Physiology,* 130**,** 2129-2141.

LANG, I., SASSMANN, S., SCHMIDT, B. & KOMIS, G. 2014. Plasmolysis: loss of turgor and beyond. *Plants (Basel),* 3**,** 583-593.

LINDEBOOM, J. J., LIOUTAS, A., DEINUM, E. E., TINDEMANS, S. H., EHRHARDT, D. W., EMONS, A. M., VOS, J. W. & MULDER, B. M. 2013. Cortical microtubule arrays are initiated from a nonrandom prepattern driven by atypical microtubule initiation. *Plant Physiology,* 161**,** 1189-1201.

LIU, Z., PERSSON, S. & SANCHEZ-RODRIGUEZ, C. 2015. At the border: the plasma membrane-cell wall continuum. *Journal of Experimental Botany,* 66**,** 1553-63.

LU, B., WANG, J., ZHANG, Y., WANG, H., LIANG, J. & ZHANG, J. 2012. AT14A mediates the cell wall-plasma membrane-cytoskeleton continuum in *Arabidopsis thaliana* cells. *Journal of Experimental Botany,* 63**,** 4061-4069.

LU, L., LEE, Y.-R. J., PAN, R., MALOOF, J. N. & LIU, B. 2005. An internal motor kinesin is associated with the Golgi apparatus and plays a role in trichome morphogenesis in *Arabidopsis*. *Molecular Biology of the Cell,* 16**,** 811-823.

MARTINIÈRE, A., GAYRAL, P., HAWES, C. & RUNIONS, J. 2011. Building bridges: formin1 of *Arabidopsis* forms a connection between the cell wall and the actin cytoskeleton. *The Plant Journal,* 66**,** 354-365.

MARTINIÈRE, A., LAVAGI, I., NAGESWARAN, G., ROLFE, D. J., MANETA-PEYRET, L., LUU, D. T., BOTCHWAY, S. W., WEBB, S. E. D., MONGRAND, S., MAUREL, C., MARTIN-FERNANDEZ, M. L., KLEINE-VEHN, J., FRIML, J., MOREAU, P. & RUNIONS, J. 2012. Cell wall constrains

lateral diffusion of plant plasma-membrane proteins. *Proceedings of the National Academy of Sciences of the United States of America,* 109**,** 12805-12810.

MCKENNA, J. F., TOLMIE, A. F. & RUNIONS, J. 2014. Across the great divide: the plant cell surface continuum. *Current Opinion in Plant Biology,* 22**,** 132-140.

MEAGHER, R. B. & FECHHEIMER, M. 2003. The *Arabidopsis* cytoskeletal genome. *The Arabidopsis Book,* 2**,** e0096. doi:10.1199/tab.0096.

MICHELOT, A., DERIVERY, E., PATERSKI-BOUJEMAA, R., GUERIN, C., HUANG, S. J., PARCY, F., STAIGER, C. J. & BLANCHOIN, L. 2006. A novel mechanism for the formation of actin-filament bundles by a nonprocessive formin. *Current Biology,* 16**,** 1924-1930.

NEBENFUHR, A., GALLAGHER, L. A., DUNAHAY, T. G., FROHLICK, J. A., MAZURKIEWICZ, A. M., MEEHL, J. B. & STAEHELIN, L. A. 1999. Stop-and-go movements of plant Golgi stacks are mediated by the acto-myosin system. *Plant Physiology,* 121**,** 1127-1141.

OPARKA, K. 1994. Plasmolysis: new insights into an old process. *New Phytologist,* 126**,** 571-591.

PAREDEZ, A. R., SOMERVILLE, C. R. & EHRHARDT, D. W. 2006. Visualization of cellulose synthase demonstrates functional association with microtubules. *Science,* 312**,** 1491-1495.

PARK, E. & NEBENFUHR, A. 2013. Myosin XIK of *Arabidopsis thaliana* accumulates at the root hair tip and is required for fast root hair growth. *PLoS One,* 8**,** 1-18.

PEREMYSLOV, V. V., KLOCKO, A. L., FOWLER, J. E., DOLJA, V. V. 2012. *Arabidopsis* myosin XI-K localizes to the motile endomembrane vesicles associated with F-actin. *Frontiers in Plant Science,* 3, 1-10.

PLESKOT, R., POTOCKY, M., PEJCHAR, P., LINEK, J., BEZVODA, R., MARTINEC, J., VALENTOVA, O., NOVOTNA, Z. & ZARSKY, V. 2010. Mutual regulation of plant phospholipase D and the actin cytoskeleton. *The Plant Journal,* 62**,** 494-507.

RASBAND, W. S. 1997-2016. ImageJ. *U. S. National Institutes of Health, Bethesda, Maryland, USA,* http://imagej.nih.gov/ij/.

RIEDL, J., CREVENNA, A., KESSENBROCK, K., YU, J., NEUKIRCHEN, D., BISTA, M., BRADKE, F., JENNE, D., HOLAK, T., WERB, Z., SIXT, M. & WEDLICH-SOLDNER, R. 2008. Lifeact: a versatile marker to visualize F-actin. *Nature Methods,* 5**,** 605-607.

ROCCHETTI, A., HAWES, C. & KRIECHBAUMER, V. 2014. Fluorescent labelling of the actin cytoskeleton in plants using a cameloid antibody. *Plant Methods,* 10**,** 1-8.

RUNIONS, J., BRACH, T., KUHNER, S. & HAWES, C. 2006. Photoactivation of GFP reveals protein dynamics within the endoplasmic reticulum membrane. *Journal of Experimental Botany,* 57**,** 43-50.

SAINT-JORE, C. M. 2001. *Green fluorescent protein to study Golgi apparatus dynamics,* PhD Thesis. Oxford Brookes University

SAMPATHKUMAR, A., GUTIERREZ, R., MCFARLANE, H. E., BRINGMANN, M., LINDEBOOM, J., EMONS, A. M., SAMUELS, L., KETELAAR, T., EHRHARDT, D. W. & PERSSON, S. 2013. Patterning and lifetime of plasma membrane-localized cellulose synthase is dependent on actin organization in *Arabidopsis* interphase cells. *Plant Physiology,* 162**,** 675-688.

SAMPATHKUMAR, A., LINDEBOOM, J. J., DEBOLT, S., GUTIERREZ, R., EHRHARDT, D. W., KETELAAR, T. & PERSSON, S. 2011. Live cell imaging reveals structural associations between the actin and microtubule cytoskeleton in *Arabidopsis*. *The Plant Cell,* 23**,** 2302-2313.

SARDAR, H. S., YANG, J. & SHOWALTER, A. M. 2006. Molecular interactions of arabinogalactan proteins with cortical microtubules and F-actin in Bright Yellow-2 tobacco cultured cells. *Plant Physiology,* 142**,** 1469-79.

SCHEIBLE, W. R., ESHED, R., RICHMOND, T., DELMER, D. & SOMERVILLE, C. 2001. Modifications of cellulose synthase confer resistance to isoxaben and thiazolidinone herbicides in *Arabidopsis Ixr1* mutants. *Proceedings of the National Academy of Sciences of the United States of America,* 98**,** 10079-10084.

SEIFERT, G. J. & BLAUKOPF, C. 2010. Irritable walls: the plant extracellular matrix and signaling. *Plant Physiology,* 153**,** 467-478.

SETHAPHONG, L., HAIGLER, C. H., KUBICKI, J. D., ZIMMER, J., BONETTA, D. T., DEBOLT, S. & YINGLING, Y. G. 2013. Tertiary model of a plant cellulose synthase. *Proceedings of the National Academy of Sciences of the United States of America,* 110**,** 7512-7517.

SHEAHAN, M., STAIGER, C., ROSE, R. & MCCURDY, D. 2004. A green fluorescent protein fusion to actin-binding domain 2 of *Arabidopsis* fimbrin highlights new features of a dynamic actin cytoskeleton in live plant cells. *Plant Physiology,* 136**,** 3968-3978.

SMERTENKO, A., DEEKS, M. & HUSSEY, P. 2010. Strategies of actin reorganisation in plant cells. *Journal of Cell Science,* 123**,** 3019-3028.

SPARKES, I. A., TEANBY, N. A. & HAWES, C. 2008. Truncated myosin XI tail fusions inhibit peroxisome, Golgi, and mitochondrial movement in tobacco leaf epidermal cells: a genetic tool for the next generation. *Journal of Experimental Botany,* 59**,** 2499-2512.

STAIGER, C., SHEAHAN, M., KHURANA, P., WANG, X., MCCURDY, D. & BLANCHOIN, L. 2009. Actin filament dynamics are dominated by rapid growth and severing activity in the *Arabidopsis* cortical array. *The Journal of Cell Biology,* 184**,** 269-280.

SZYMANSKI, D. B. & COSGROVE, D. J. 2009. Dynamic coordination of cytoskeletal and cell wall systems during plant cell morphogenesis. *Current Biology,* 19**,** 800-811.

TATENO, M., BRABHAM, C. & DEBOLT, S. 2016. Cellulose biosynthesis inhibitors - a multifunctional toolbox. *Journal of Experimental Botany,* 67**,** 533-542.

VAN DER HONING, H. S., VAN BEZOUWEN, L. S., EMONS, A. M. & KETELAAR, T. 2011. High expression of Lifeact in *Arabidopsis thaliana* reduces dynamic reorganization of actin filaments but does not affect plant development. *Cytoskeleton (Hoboken),* 68**,** 578-587.

WANG, P., HAWKINS, T. J., RICHARDSON, C., CUMMINS, I., DEEKS, M. J., SPARKES, I. A., HAWES, C. & HUSSEY, P. J. 2014. The plant cytoskeleton, NET3C, and VAP27 mediate the link between the plasma membrane and endoplasmic reticulum. *Current Biology,* 24**,** 1397-1405.

WILSON, S. M., HO, Y. Y., LAMPUGNANI, E., VAN DE MEENE, A. M., BAIN, M. P., BACIC, A. & DOBLIN, M. S. 2015. Determining the subcellular location of synthesis and assembly of the cell wall polysaccharide (1,3; 1,4)-β-D-glucan in grasses. *The Plant Cell,* 27**,** 754-771.

WOJTASZEK, P., BALUSKA, F., KASPROWICZ, A., LUCZAK, M. & VOLKMANN, D. 2007. Domain-specific mechanosensory transmission of osmotic and enzymatic cell wall disturbances to the actin cytoskeleton. *Protoplasma,* 230**,** 217-230.

ZHU, C., GANGULY, A., BASKIN, T. I., MCCLOSKY, D. D., ANDERSON, C. T., FOSTER, C., MEUNIER, K. A., OKAMOTO, R., BERG, H. & DIXIT, R. 2015. The fragile Fiber1 kinesin contributes to cortical microtubule-mediated trafficking of cell wall components. *Plant Physiology,* 167**,** 780-792.

Table 1. Actin cytoskeleton Bulk Remodelling Index (BRI) of cells labelled with GFP-FABD2. Plasmolysis was done using 0.6M mannitol for 30 min. Subsequent rehydration of cells was done with dH_2O for 30 min. BRI was quantified using *Pairwise image subtraction*. Eight plants per treatment x 4-5 cells/plant x 19 BRI values per cell. SD=standard deviation.

GFP-FABD2	**Bulk remodelling index**		
	Control	**Plasmolysed**	**Rehydrated**
Number of BRI values	665	570	760
Mean ± SD	0.56 ± 0.06	0.53 ± 0.04*	0.60 ± 0.09
Lower and upper 95% confidence interval	0.55 – 0.56	0.52 – 0.53	0.59 – 0.61

* BRI in plasmolysed cells was significantly lower than in both control and rehydrated cells ($p<0.0001$).

Table 2. Actin cytoskeleton bulk remodelling of cells labelled with GFP-Lifeact; non-treated control compared to plasmolysed and rehydrated cells. Cumulative fluorescence intensity (CFI) values were measured using *Cumulative fluorescence intensity.* Plasmolysis was done using 0.6M mannitol for 30 min. Mean and standard deviation of all CFIs in Table S1. Six plants per treatment x >25 cells/plant.

Cumulative fluorescence intensity value	p-value from One-way ANOVA	p-value from Tukey post-test for control vs plasmolysed
17	0.0192 *	$p < 0.05$
18	0.0209 *	$p < 0.05$
19	0.0093 **	$p < 0.01$

*$p < 0.05$ and **$p < 0.01$.

Table 3. Actin cytoskeleton bulk remodelling estimated via the proxy of Golgi body motility. Cells labelled with ST-GFP and Golgi body movement tracked using Volocity software. Plasmolysis was done using 0.6M mannitol for 30 min. Subsequent rehydration of cells was done with dH_2O for 30 min. Seven plants per treatment x approx 5 cells/plant.

	Control	**Plasmolysed**	**Rehydrated**
Number of Golgi bodies tracked	910	848	626
Average velocity (Mean ± SEM)	0.69 ± 0.02 µm/s	0.52 ± 0.02 µm/s *	0.77 ± 0.02 µm/s
Displacement rate (Mean ± SEM)	0.28 ± 0.01 µm/s	0.21 ± 0.01 µm/s *	0.34 ± 0.02 µm/s
Meandering index (Mean ± SD)	0.33 ± 0.25	0.28 ± 0.26 *	0.35 ± 0.27
Number of time frames in view (Mean ± SD)	46 ± 44	76 ± 58 *	53 ± 47 *

**p<0.001

Figure legends

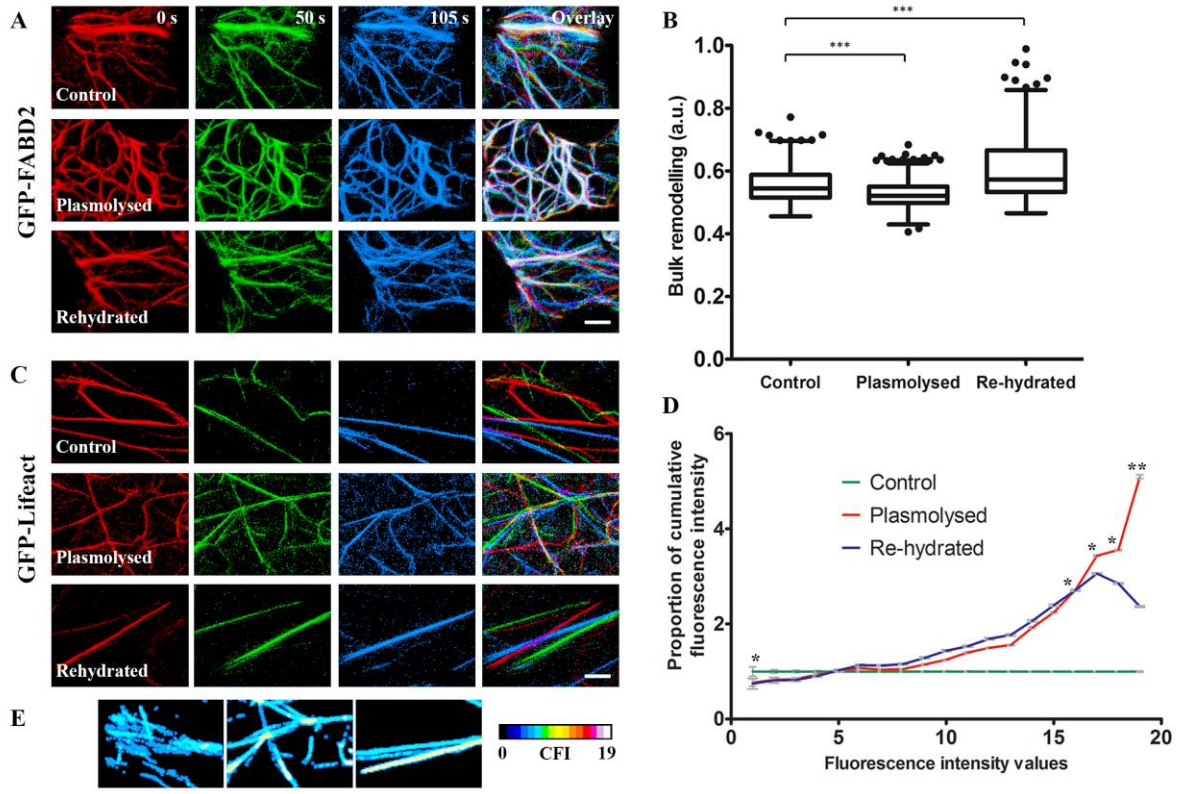

Figure 1. Disruption of the cell wall-plasma membrane interface alters the dynamic remodelling of the actin cytoskeleton. Plasmolysis was done using 0.6M mannitol for 30 min. Subsequent rehydration of cells was done with dH_2O for 30 min. Seven plants per experiment x 4-5 cells/plant. Scale bar = 5 µm. (A) GFP-FABD2 labelled actin cytoskeleton of control, plasmolysed and rehydrated cells at three time-points: 0 s (red), 50 s (green) and 105 s (blue), the fourth image is a merge of the previous three and indicates visually the amount of actin remodelling that has occurred. (B) Box plot of Bulk Remodelling Index (BRI) of GFP-FABD2 networks, calculated using *Pairwise image subtraction*, the index is lower for more static networks. The data were compared using an unpaired t-test with Welch's correction, ***p < 0.001, only p-values relating to the control are shown. (C) GFP-Lifeact labelled actin cytoskeleton of control, plasmolysed and rehydrated cells at three time-points: 0 s (red), 50 s (green) and 105 s (blue), the fourth image is a merge of the previous three and indicates visually the amount of actin remodelling that has occurred. (D) Cumulative fluorescence intensity (CFI) values of GFP-Lifeact networks calculated using *Cumulative fluorescence intensity*, a higher proportion at higher CFI values indicates a more static network, whilst a higher proportion at a lower CFI values means a more dynamic network. All conditions are

expressed as a ratio compared to the control, hence the control itself is always one. Mean ± SD. The data were compared using one-way ANOVA with a Tukey post-test, *p < 0.05, **p < 0.01, only p-values relating to the control are shown. (E) Timeseries of GFP-Lifeact labelled actin cytoskeleton in control, plasmolysed and re-hydrated cells visualised using *Cumulative fluorescence intensity*. 20 time frames have been superimposed to produce each image and the colour in these heat-maps represents the amount of remodelling that has occurred during the 105 seconds of observation. Blue represents relatively high rates of bulk remodelling (more pixel locations at low CFI) and orange/red represent relatively low rates of bulk remodelling (more pixel locations at high CFI). The heat map scale used to indicate CFI (0-19) is on the right.

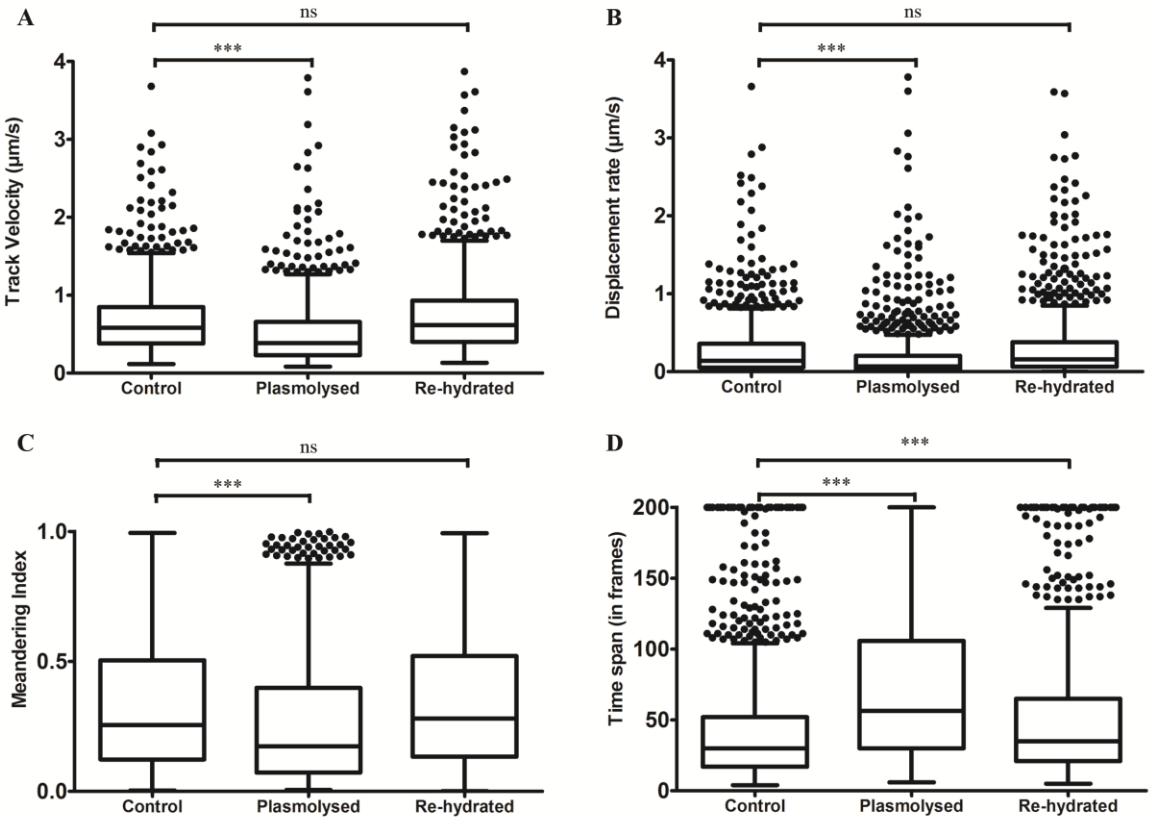

Figure 2 Disruption of the cell wall-plasma membrane interface alters Golgi body motility. Plasmolysis was done using 0.6M mannitol for 30 min. Subsequent rehydration of cells was done with dH_2O for 30 min. Seven plants per experiment x 4-5 cells/plant. (A-D) Golgi body motility indicies quantified using Volocity software. (A) Average track velocity of Golgi bodies (µm/sec). Golgi bodies move significantly more slowly in plasmolysed cells relative to control

and rehydrated cells. The data were compared using the Kruskal-Wallis test with Dunn's multiple comparison test. (B) Average displacement rate, calculated as the length of time taken to travel between two points (µm/sec). Golgi bodies displace significantly more slowly in plasmolysed cells relative to control and rehydrated cells. The data were compared using the Kruskal-Wallis test with Dunn's multiple comparison test. (C) Meandering index, calculated as the ratio between the average displacement rate and the average velocity. Golgi bodies movement is significantly more saltational in plasmolysed cells relative to control and rehydrated cells. The data were compared using the Kruskal-Wallis test with Dunn's multiple comparison test. (D) Time span (frames) that Golgi bodies remain in the field of view. Golgi bodies remain static significantly longer in plasmolysed cells and rehydrated cells relative to control cells. The data were compared using an unpaired t-test with Welch's correction, **p < 0.01 and ***p < 0.001, only p-values relating to the control are shown.

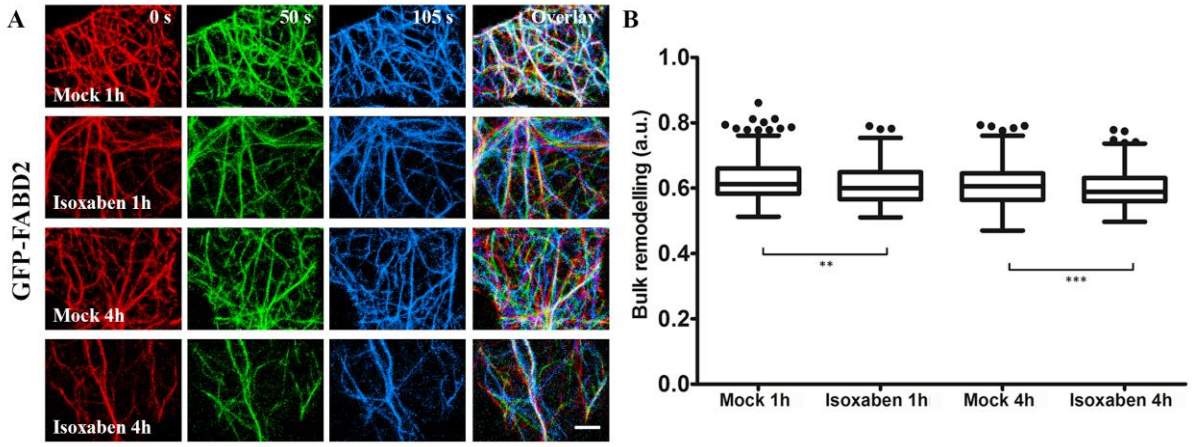

Figure 3 Isoxaben, a cell-wall specific disruptor, alters the dynamic remodelling of the actin cytoskeleton. Leaf tissue was treated in 20 µM isoxaben for either 1 hour or 4 hours. Bulk Remodelling Index of cells labelled with GFP-FABD2. BRI was quantified using *Pairwise image subtraction*. Seven plants per treatment x 4-5 cells/plant x 19 BRI values per cell. Scale bar = 5 µm. (A) GFP-FABD2 labelled actin cytoskeleton in control-, and isoxaben-treated cells at three time-points: 0 s (red), 50 s (green) and 105 s (blue), the fourth image is a merge of the previous three and indicates visually the amount of actin remodelling that has occurred. (B) Box plot of Bulk Remodelling Index, calculated using *Pairwise image subtraction*, the index is lower for networks that are more static. Isoxaben-treatment resulted in significantly reduced

BRI after both 1 hour and 4 hours relative to controls. The data were compared using the Kruskal-Wallis test with Dunn's multiple comparison test, **p < 0.01 and ***p < 0.001, only p-values relating to the control are shown on the figure.

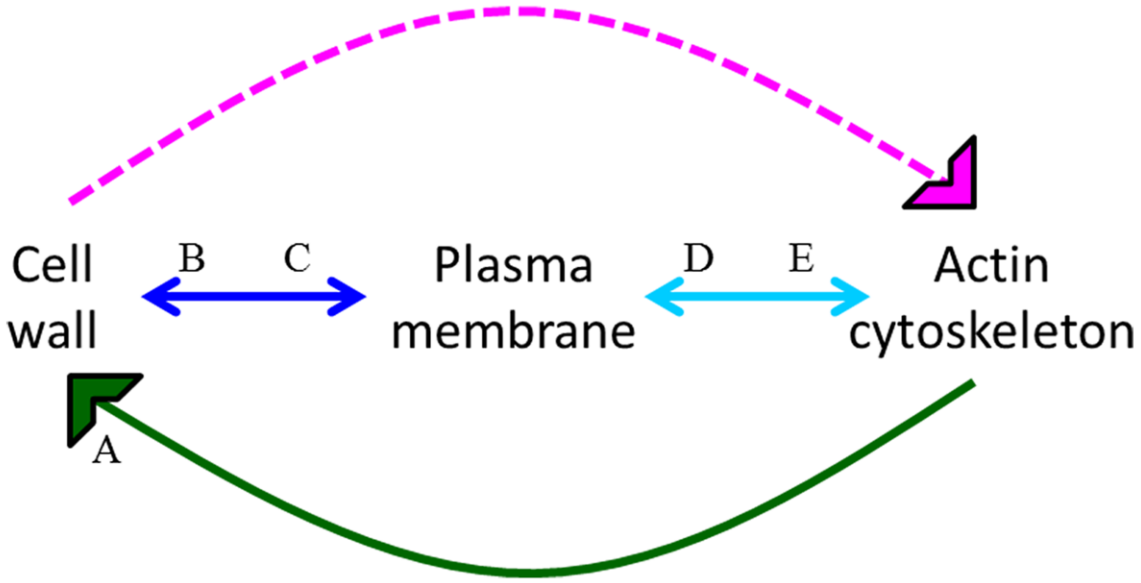

Figure 4. Schematic showing the interactions in the continuum.

The direction of the arrow shows what is being influenced. Known regulations are solid lines, whilst the one investigated during the course of this study are highlighted with a dotted line. A) Actin influence on cell wall (Sampathkumar *et al.*, 2013); B) Plasma membrane influence on cell wall (Kohorn and Kohorn, 2012); C) Cell wall influence on plasma membrane (Martinière *et al.,* 2012); D) Actin influence on plasma membrane (Gowrishankar *et al.,* 2012); E) Plasma membrane influence on Actin (Pleskot *et al.,* 2010) and Martinière *et al.* (2011).

Supplemental data

Table S1. Actin cytoskeleton bulk remodelling in cells with different plasmolysis treatments visualised with GFP-Lifeact. The proportion of *Cumulative fluorescence intensity* (mean ± standard deviation) at each of 19 CFI levels. Each data column sums to 1.000. A reduction in CFI at higher fluorescence intensity levels (17-19), such as happens when the Control cells are compared to Plasmolysed cells, implies that the network has become more static as a result of the treatment.

Fluorescence intensity level	Proportion of CFI at each fluorescence intensity level		
	Control	Plasmolysed	Re-hydrated
1	0.2695 ± 0.09911	0.2063 ± 0.07478	0.2007 ± 0.11160
2	0.1647 ± 0.03782	0.1360 ± 0.03988	0.1338 ± 0.05890
3	0.1209 ± 0.02862	0.1015 ± 0.02916	0.0994 ± 0.03314
4	0.0880 ± 0.02181	0.0825 ± 0.02142	0.0794 ± 0.02296
5	0.0683 ± 0.01434	0.0686 ± 0.01458	0.0699 ± 0.02128
6	0.0553 ± 0.01502	0.0592 ± 0.01094	0.0625 ± 0.02068
7	0.0472 ± 0.01579	0.0490 ± 0.00780	0.0531 ± 0.01877
8	0.0401 ± 0.01590	0.0421 ± 0.00948	0.0463 ± 0.01913
9	0.0319 ± 0.01356	0.0366 ± 0.01204	0.0410 ± 0.01973
10	0.0256 ± 0.01214	0.0320 ± 0.01361	0.0368 ± 0.02011
11	0.0207 ± 0.01177	0.0289 ± 0.01424	0.0316 ± 0.02151
12	0.0166 ± 0.01060	0.0248 ± 0.01408	0.0279 ± 0.02255
13	0.0136 ± 0.01020	0.0212 ± 0.01421	0.0240 ± 0.02248
14	0.0100 ± 0.00820	0.0193 ± 0.01404	0.0207 ± 0.02314
15	0.0074 ± 0.00759	0.0167 ± 0.01318	0.0178 ± 0.02225
16	0.0058 ± 0.00719	0.0157 ± 0.01365	0.0156 ± 0.02079
17	0.0044 ± 0.00674	0.0151 ± 0.01403	0.0135 ± 0.01718
18	0.0042 ± 0.00750	0.0150 ± 0.01367	0.0120 ± 0.01500
19	0.0059 ± 0.01500	0.0298 ± 0.03793	0.0138 ± 0.01871

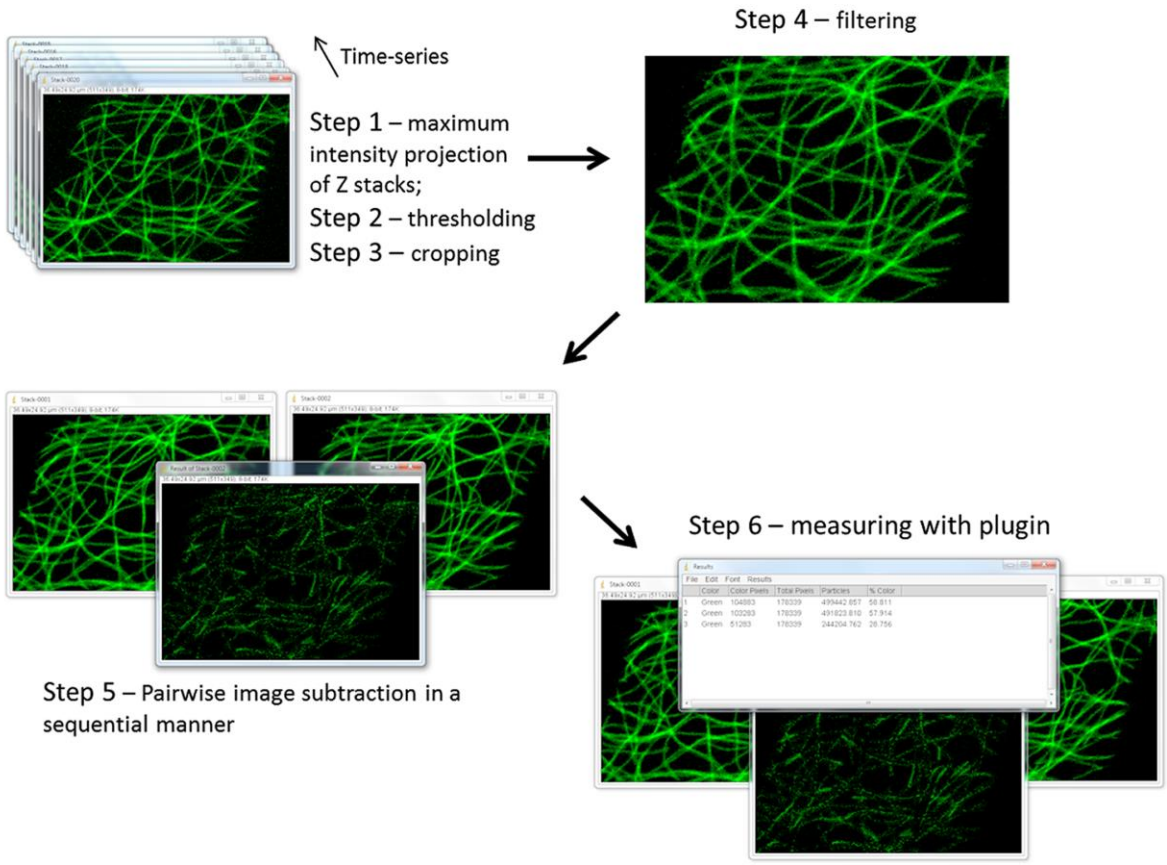

Figure S1. Workflow for *Pairwise image subtraction*. Steps 1 - 3 detail production of maximum intensity projections of all the Z-stacks within the 3D time-series followed by thresholding so that the background has a value of '0' and finally cropping so all images are 200 by 150 pixels (30,000 pixels in total). In step 4 the time-series are filtered using a median filter of size 0.2. Step 5 is sequential subtraction using the 'Image calculator' in ImageJ. The resultant subtracted image is a representation of all actin cytoskeleton movement that has occurred during the inter-frame interval. Lastly, Step 6 is the use of the plugin 'Color Pixel Counter' that counts the number of pixels containing a fluorescent intensity above a set value and produces a log window with the results. The number of fluorescent pixels in the subtracted image is then compared to the number of fluorescent pixels in the first image of the pair being tested to arrive at a Bulk Remodelling Index (BRI) value. A small BRI value indicates little remodelling occurred, while larger BRI values indicate a very dynamic actin network.

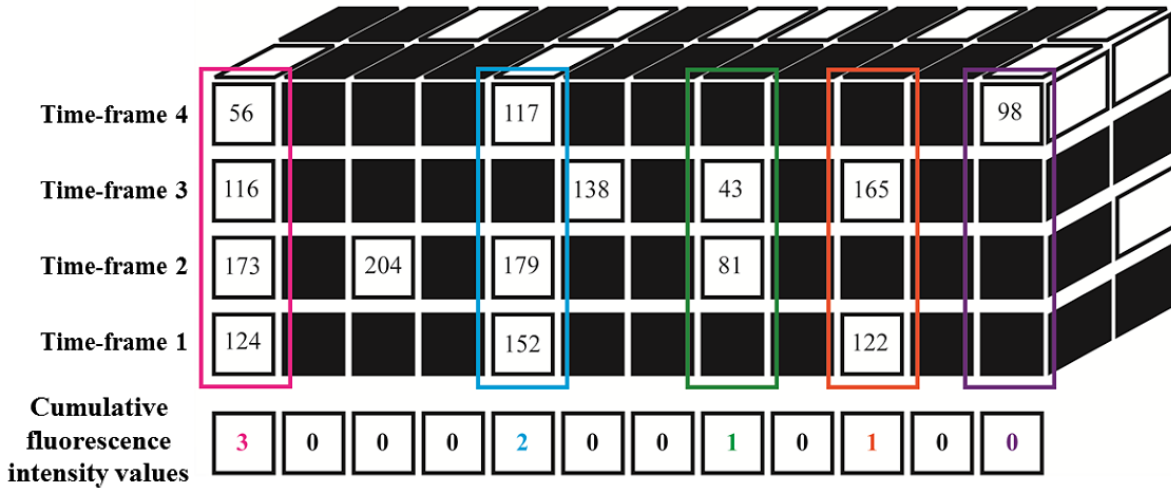

Figure S2. Schematic of the *Cumulative fluorescence intensity* analysis technique. This schematic presents a 3D array of pixels (xyt). A z-stack is collected at each time-point and maximally projected, although this is not essential, only x and y information is necessary per time-frame. Maximum projection images are processed as for *Pairwise image subtraction* to the median filtering step (Fig. S1 - Step 4). Each pixel location is then tested for fluorescence, the numbers in the white boxes indicate some level of fluorescence between 1–255, e.g. 56 in the top left pixel (time-frame 4); although the amount of fluorescence is irrelevant. All pixels with fluorescence intensity >0 are then assigned a value of '1' and pixels with no fluorescence are assigned a value of '0'. Assigned values are then summed down columns to arrive at the Cumulative fluorescence intensity (CFI) value for that pixel location across the entire time-series. The first value of '1' in each column is not counted in this calculation to remove residual noise. The CFI for each pixel location in this scheme is displayed in a box below the pixel location. The pink box on the left outlines a pixel that contains signal at every time-frame in the time-series. CFI=3 in this case.

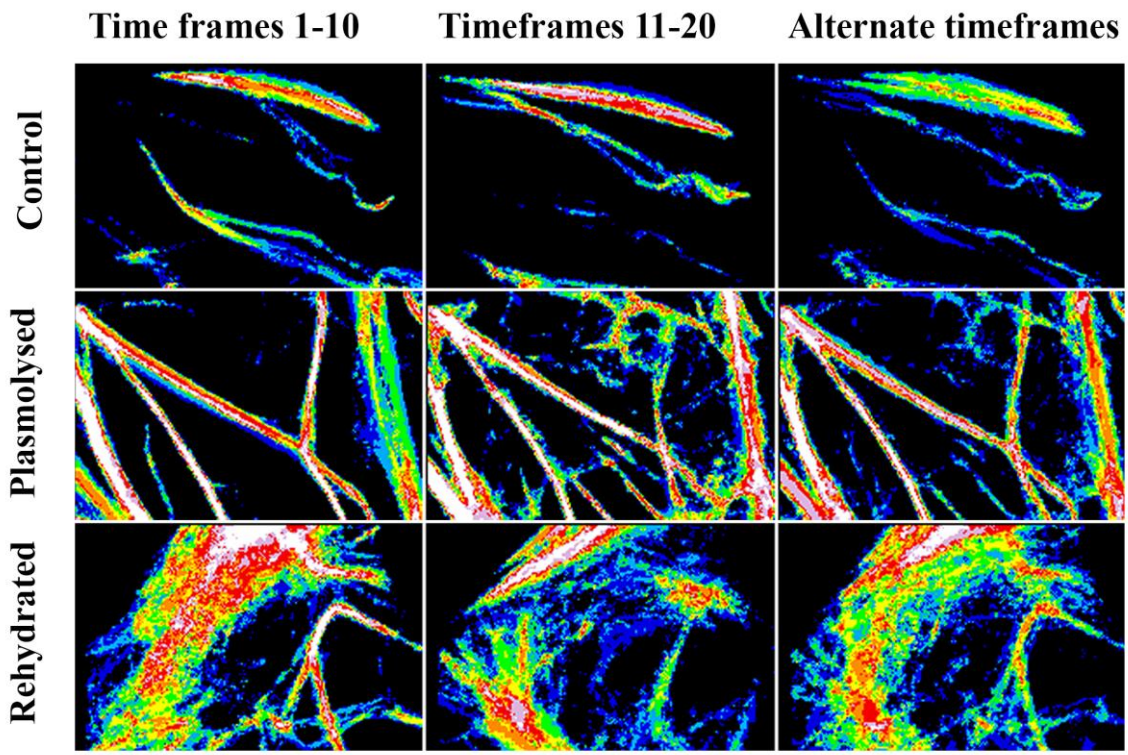

Figure S3. Validation of the *Cumulative fluorescence intensity* analysis using a modified 'bootstrapping' method. Timeseries images superimposed and Cumulative fluorescence intentity (CFI) values colour-coded (blue=low CFI, green=medium CFI, and white=high CFI). The first column shows the results from the *Cumulative fluorescence intensity* analysis using only the first ten images from a timeseries and the second column is the last ten images from a timeseries. The third column shows the results from the *Cumulative fluorescence intensity* analysis using every second image from a timeseries so that it appears to be running double speed. When the data were normalised, it showed that there was an increase in the proportion of pixels at the highest CFI values for the plasmolysed timeseries (middle row) which indicated that the actin network had become more static as a result of the treatment.

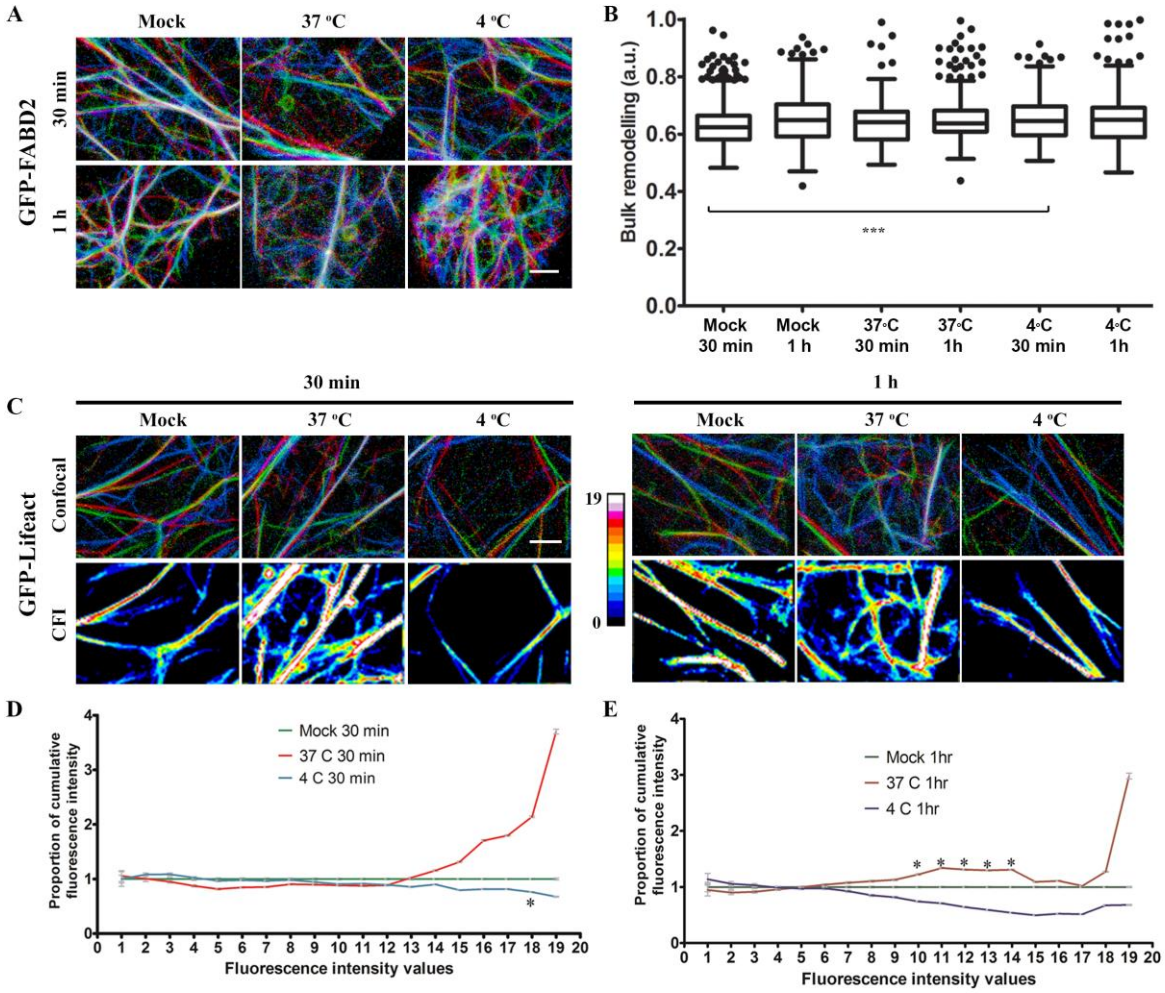

Figure S4. Temperature stress does not alter the dynamic remodelling of the actin cytoskeleton. (A and C) Actin cytoskeleton at three time-points that have been re-coloured and merged: 0 s (red), 50 s (green) and 105 s (blue). These represent the two image analyses techniques that have been used to quantify network re-modelling. (A) GFP-FABD2 labelled actin cytoskeleton in cells incubated at room temperature (mock), 37 °C and 4 °C. (B) Box plot of bulk remodelling index of GFP-FABD2 networks, calculated using *Pairwise image subtraction*, the index is lower for networks that are more static. Here, the only significant difference measured was the increase in BRI relative to controls in cells treated at 4°C for 30 min. (C) GFP-Lifeact labelled actin cytoskeleton in cells incubated at room temperature (mock), 37 °C and 4 °C, for either 30 min or 1 hour. Bulk remodelling was quantified using *Cumulative fluorescence intensity* and the bottom row of micrographs illustrate CFI colour-coding as per the included scale (blue=low CFI, green=medium CFI, and white=high CFI). (D-E) The proportion of CFI at each of 19 possible levels relative to control levels which have

been normalised to ‘1’. A higher proportion at the higher CFI levels indicates a more static network. Asterisks indicate significant differences between the indicated treatment and controls. The significant decrease in CFI at level 18 in the 4°C 30 min treatment correlates with the increased BRI found in this treatment using *Pairwise image subtraction* of GFP-FABD2 labelled timeseries. 5 - 7 plants per treatment x 4-5 cells/plant. *p < 0.05 and ***p < 0.001, only p-values relating to the control are shown in D and E. Scale bar = 5 µm.

Movie S1. GFP-FABD2 labelled actin cytoskeleton dynamics. Timelapse = 30s.

Movie S2. GFP-Lifeact labelled actin cytoskeleton dynamics. Timelapse = 30s.